

# Longitudinal top quark polarization

Małgorzata Awramik<sup>a</sup>, Marek Jeżabek<sup>b</sup>

<sup>a</sup>*Department of Field Theory and Particle Physics,  
University of Silesia,  
Uniwersytecka 4, PL-40007 Katowice, Poland*

<sup>b</sup>*Institute of Nuclear Physics,  
Kawiorzy 26 a, PL-30055 Cracow, Poland*

## Abstract

Longitudinal polarization of the top quark, averaged over the production angle, is discussed for the top quark produced in  $e^+e^-$  annihilation near its production threshold. It is demonstrated that Coulomb type corrections and rescattering corrections are important. They change considerably measurable quantities and should be taken into account in phenomenological analysis.

PACS numbers: 13.88.+e, 14.65.Ha

# 1 Introduction

The heaviest of all known elementary particles, the top quark, is likely to give us exciting insight into the electroweak symmetry breaking sector of the Standard Model (SM), into QCD dynamics at short distances and maybe even into physics beyond the SM. Precise measurements not only of the total top quark production cross section, but also of the top quark momentum distributions and polarizations are planned to be carried out at a future linear electron-positron collider. Of particular interest is the subject of top-antitop production close to threshold. For the large width of the top quark  $\Gamma_t$  [1] a formalism suitable for this region, where the strong interaction between  $t$  and  $\bar{t}$  due to Coulomb-like gluons is of paramount importance, was suggested by V.S. Fadin and V.A. Khoze [2]. It is based on solving Schrödinger equation for Green functions in a non-relativistic approximation for a Coulombic potential. The methods needed for the calculation of the total cross section were first given in [1] and [3]. The differential top quark distributions were calculated independently in position space [4, 5] and by solving Lippmann-Schwinger equations in momentum space [6, 7]. The polarization of the top quark has been considered in [8, 9]. In [10, 11] rescattering corrections (between  $t\bar{t}$  and the decay  $b$  and  $\bar{b}$  quarks) to order  $\mathcal{O}(\alpha_s)$  were included<sup>1</sup>.

One of the interesting quantities is the top quark longitudinal polarization. It has been claimed in [15] that it may easily provide information on the mass and width of the top quark, independently of Coulomb type corrections and of the running of the strong coupling  $\alpha_s$ . However, in this article we demonstrate that the helicity of the top quark significantly depends on Coulomb type corrections. Moreover, we show that some easily measurable quantities related to the top net helicity strongly depend on rescattering corrections and therefore it requires a more careful analysis to extract from them some information on top quark parameters. Although the NNLO QCD corrections to the total and differential cross section (excluding rescattering corrections) for the top quark production in the electron-positron annihilation are already known (see [16] and [17]; recent results are given in [18]), polarization has not yet been introduced. A major problem is caused by the rescattering corrections since the inclusion of the interactions between relativistic ( $b$  quark) and non-relativistic ( $t$  quark) states is difficult within

---

<sup>1</sup>For a review and references see e.g. [12, 13, 14]

this formalism.

In section 2 we investigate the top quark net helicity when rescattering corrections are neglected. We show that large Coulomb type corrections affect this observable, in contradiction to the statements made in [15]. For unstable quarks, the polarization is a function of the momentum and energy independently<sup>2</sup>. To compare our results to [15] we need some averaging procedure. We show, however, that differences persist in two intuitively acceptable approaches. Inclusion of the phenomenological potential  $V_{JKT}$  (see [6]) with the two loop static potential, running of the strong coupling constant and a Richardson-like potential for small momenta leads to further deviations from [15].

In section 3, we note that the top quark average helicity is not directly observable. Following [9] we derive an analogue from the leptonic distributions, taking a more suitable choice of basis vectors. We show, however, that the latter quantities are significantly affected by the final state interactions.

Our conclusions are presented in section 4.

The Appendix contains the formulas necessary to express the observables of [9] in a basis aligned with the top quark momentum.

## 2 Coulomb corrections and finite width

We start from the definition of the angular average of the top quark polarization

$$\langle \mathcal{P} \rangle = \frac{\int \mathcal{P} \frac{d\sigma}{dp d\Omega_p} d\Omega_p}{\int \frac{d\sigma}{dp d\Omega_p} d\Omega_p} \quad (1)$$

where  $\frac{d\sigma}{dp d\Omega_p}$  is the momentum distribution of the top quark and  $\mathcal{P}$  its polarization. The angular average of the longitudinal polarization is

$$\langle \mathcal{P}_L \rangle = \frac{4}{3} C_{\perp} \varphi_R \quad (2)$$

where  $C_{\perp}$  is a well known function of the electroweak couplings of the t quark to the photon and  $Z^0$ . In Appendix A we give a derivation of Eq. (2) using the results of [8] and [9]. An explicit formula for  $C_{\perp}$  is given therein, see

---

<sup>2</sup>We take the energy with reference to the nominal threshold  $E = \sqrt{s} - 2m_t$

Eq. (27). The function  $\varphi_R = Re(\varphi)$  originates from the interference of the  $S$  and  $P$  wave production

$$\varphi(p, E) = \frac{(1 - 4\alpha_s/3\pi) p F^*(p, E)}{(1 - 8\alpha_s/3\pi) m_t G^*(p, E)}. \quad (3)$$

The functions  $G$  and  $F$  correspond to the respective waves and are found numerically by solving the Lippmann-Schwinger equations.

For stable and non-relativistic quarks and assuming a pure Coulomb potential  $G$  and  $F$  can be found analytically [19]. Following the remarks in [19] and [9] we rewrite Eq. (3) as

$$\lim_{\Gamma_t \rightarrow 0, E \rightarrow \frac{p^2}{m_t}} \varphi_R \equiv \varphi_0 = \frac{(1 - 4\alpha_s/3\pi)}{(1 - 8\alpha_s/3\pi)} \beta. \quad (4)$$

Here  $\beta = \sqrt{1 - 4m_t^2/s}$  is the on-shell top quark velocity. In this limit the longitudinal top polarization is given by

$$\lim_{\Gamma_t \rightarrow 0, E \rightarrow \frac{p^2}{m_t}} \langle \mathcal{P}_L \rangle \equiv \langle \mathcal{P}_0 \rangle = \frac{4}{3} C_\perp Re(\varphi_0). \quad (5)$$

In Fig. 1 we show how Eq. (1) approximates to Eq. (5) as  $\Gamma_t$  decreases. Although the momentum distributions are getting narrower to simulate the Dirac delta function, the limiting value of the polarization of Eq. (1) is reproduced only in the near vicinity of the peak.

In [15], the Eq. (5) was used as a starting point. The finite width was taken into account by changing the dispersion relation

$$p = \sqrt{m_t(E + i\Gamma_t)}, \quad (6)$$

which leads to the longitudinal top polarization

$$\langle \langle \mathcal{P}_L \rangle \rangle_S = \frac{4}{3} \left(1 + \frac{4\alpha_s}{3\pi}\right) C_\perp Re\left(\sqrt{\frac{E + i\Gamma_t}{m_t}}\right). \quad (7)$$

In a more complete analysis the width is accounted for by momentum distributions. Therefore a comparison with Eq. (7) requires some averaging. We

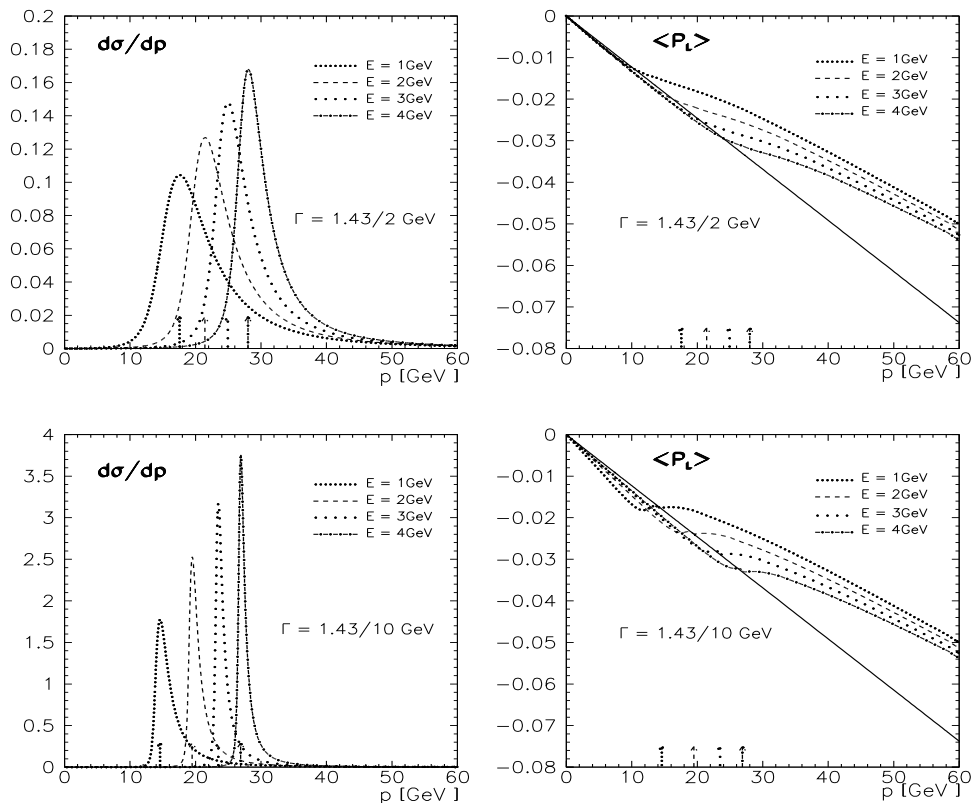


Figure 1: On the left: top quark momentum distributions  $d\sigma/dp$ . On the right: the polarization  $\langle \mathcal{P}_L \rangle$  from the  $S$ - $P$  wave interference term shown for several different energies, compared with  $\langle \mathcal{P}_0 \rangle$  (solid lines). The upper plots show the dependence for an artificially small width  $\Gamma_t \rightarrow \Gamma_t/2$ , the lower are for  $\Gamma_t \rightarrow \Gamma_t/10$ . The arrows indicate the peak of the momentum distribution. We have chosen  $m_t = 175$  GeV,  $\Gamma_t = 1.43$  GeV. We use the pure Coulomb potential with  $\alpha_s$  fixed at average value of the peak momentum  $\alpha_s(p = 20) = 0.15$ .

shall consider two possibilities. In Fig. 2 we take the value of the polarization at the peak of the momentum distribution as function of the energy. In Fig. 3, we show the average

$$\langle \langle \mathcal{P} \rangle \rangle = \frac{\int_0^{p_{max}} \mathcal{P} \frac{d\sigma}{dp d\Omega_p} d\Omega_p dp}{\int_0^{p_{max}} \frac{d\sigma}{dp d\Omega_p} d\Omega_p dp} \quad (8)$$

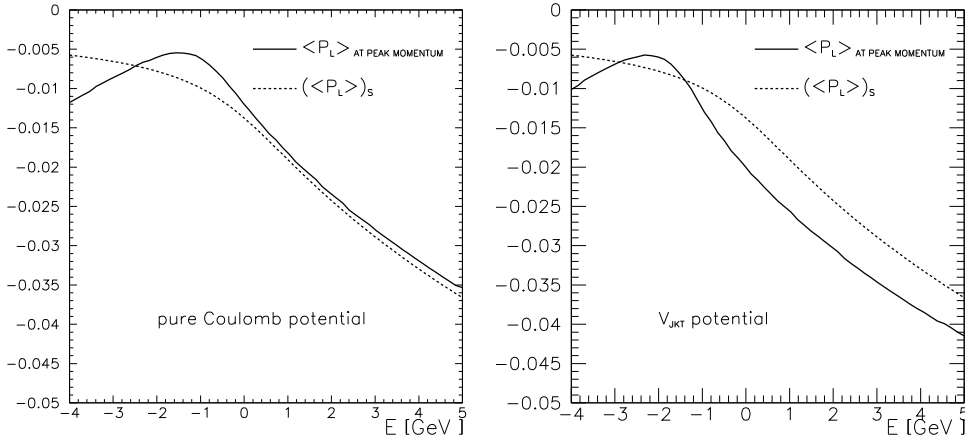


Figure 2: Longitudinal polarization  $\langle \mathcal{P}_L \rangle$  (solid line) taken at the peak of the momentum distribution for the pure Coulomb potential (left) and phenomenological potential  $V_{JKT}$  (right) compared with  $\langle \langle \mathcal{P}_L \rangle \rangle_s$  (dashed line).

for the longitudinal part of the top polarization

$$\langle \langle \mathcal{P}_L \rangle \rangle = \frac{\int_0^{p_{max}} \langle \mathcal{P}_L(p, E) \rangle |p G(p, E)|^2 dp}{\int_0^{p_{max}} |p G(p, E)|^2 dp}. \quad (9)$$

Due to the non-relativistic approximation employed in our calculation of the Green functions  $F$  and  $G$ ,  $\langle \langle \mathcal{P}_L \rangle \rangle$  increases logarithmically with  $p_{max}$ . We show the results for two values of the cut off,  $p_{max} = \frac{2}{3}m_t$  and  $p_{max} = \frac{1}{4}m_t$ . The former cut off corresponds to more than 97% of the total cross section in the energy range between 1S peak and  $E = 5$  GeV. In the latter case about 80% of the total cross section is included. So our calculation should be compared with the data sample for a corresponding cut off.

For a pure Coulomb potential and positive energies the formula (7) can be reproduced, as shown in Fig. 2a and Fig. 3a. However for negative energies in the region of the 1S peak there are significant differences.

A further improvement in the analysis can be obtained by including the phenomenological potential [6]. This is shown in Fig. 2b and Fig. 3b. This time the normalization of the curves is significantly different even in the

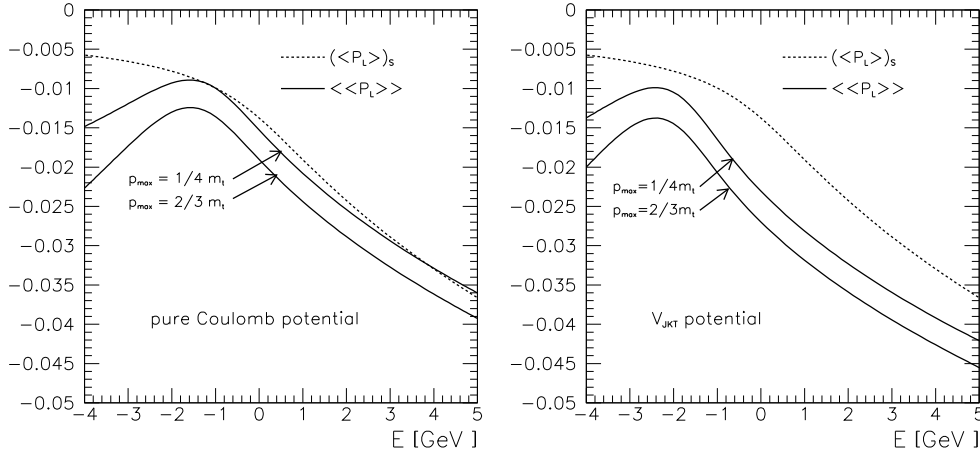


Figure 3: Angular and momentum average of the longitudinal top quark polarization  $\langle\langle\mathcal{P}_L\rangle\rangle$  for the pure Coulomb potential (left) and  $V_{JKT}$  (right) shown in comparison with  $\langle\langle\mathcal{P}_L\rangle\rangle_s$ .

positive energy region.

We think that the polarization at 1S peak is sensitive to both, the top quark width  $\Gamma_t$  and  $\Delta E_{1S-2P}$  energy difference between 1S and 2P peak values. The formula (7) is not sensitive to  $\Delta E_{1S-2P}$  and hence in our opinion cannot be considered a very good approximation.

### 3 Rescattering corrections

Due to the extremely short life time of the top quark it will never be possible to carry out any experiment directly on it. The most suitable way of determining the observables discussed here is based on the analysis of charged leptons from the semileptonic decay channel:  $e^+ e^- \rightarrow t \bar{t} \rightarrow b l \nu \bar{b} W^-$ . The average of the charged lepton distribution is relatively easy to settle theoretically as well as experimentally

$$\langle nl \rangle \equiv \left( \frac{d^3\sigma}{dp d\Omega_p} \right)^{-1} \int dE_l d\Omega_l \frac{d\sigma(e^+ e^- \rightarrow b l \nu \bar{b} W^-)}{dp d\Omega_p d\Omega_l dE_l} (nl), \quad (10)$$

where  $l$  is the four-momentum of the charged lepton and  $n$  is a chosen unit four-vector. In [9] it was calculated as

$$\langle nl \rangle = \text{BR}(t \rightarrow bl\nu) \frac{1 + 2y + 3y^2}{4(1 + 2y)} \left[ (tn) + \frac{m_t}{3} (n\mathcal{P}) \right]. \quad (11)$$

In the  $t\bar{t}$  center-of-mass frame  $t^\mu = (m_t, \mathbf{p})$  is the top quark four-momentum and  $y = \frac{m_W^2}{m_t^2}$ . The components of  $\mathcal{P}$  turn out to be identical with those of the top quark polarization originating from the S-P wave interference in the  $e^+e^- \rightarrow t\bar{t}$  process. Thus we consider  $\mathcal{P}$  to represent the polarization.

In [9] it was also shown that the largest known corrections to  $\langle nl \rangle$  arise from the color interaction between bottom and antitop quarks (or top and antibottom). An intuitive picture is given in [10] and [11]. Corrections due to this effect are called 'rescattering corrections', or 'final-state corrections', or 'non-factorizable corrections'. It is known that they almost disappear in the total cross sections but they modify the differential distributions ([5], [9]). We implement them in our approach in the same way as we did before (see Appendix A). Then the longitudinal top quark polarization, the polarization perpendicular to the top quark momentum and normal to the production plane averaged over the angles are respectively:

$$\langle \mathcal{P}_L \rangle = \frac{4}{3} C_\perp \varphi_R + \frac{1}{3} k_1 \text{Re}(\Psi_2), \quad (12)$$

$$\langle \mathcal{P}_T \rangle = -\frac{\pi}{4} C_\parallel^0 + \frac{\pi}{16} k_2 C_\parallel^0 \Psi_3, \quad (13)$$

$$\langle \mathcal{P}_N \rangle = \frac{\pi}{4} C_N \text{Im}(\varphi), \quad (14)$$

where

$$k_1 = 2 \frac{3(1 - 3y^2)}{2(1 + 2y + 3y^2)} + \frac{2 + 3y - 5y^2 - 12y^3}{(1 + 2y)(1 + 2y + 3y^2)}, \quad (15)$$

$$k_2 = -2 \frac{3(1 - 4y + 3y^2)}{8(1 + 2y + 3y^2)} - \frac{1 - 4y + 3y^2}{4(1 + 2y + 3y^2)}. \quad (16)$$

The functions  $\Psi_2$  and  $\Psi_3$  (see [9]) are connected with the rescattering corrections in the  $t\bar{b}$  system and appear to be of the same order of magnitude. For  $m_t = 175$  GeV the coefficients  $k_i$  are:  $k_1 = 2.7$  and  $k_2 = -0.19$  so the corrections to the longitudinal polarization are proportional to  $0.9 \text{Re}(\Psi_2)$  and

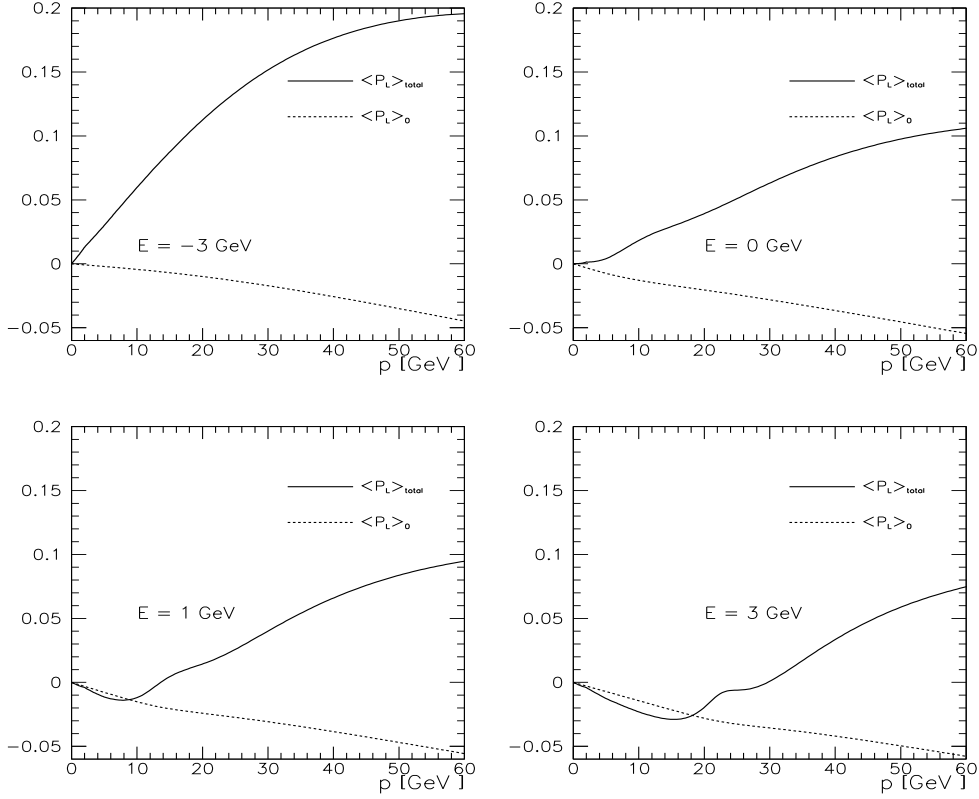


Figure 4: Angular average of the longitudinal top polarization with rescattering  $\langle P_L \rangle$  (solid line), compared with the S-P wave interference term (dotted line), for several different energies.

to the perpendicular polarization:  $0.04 \Psi_3$ . Thus the perpendicular and the normal components of the polarization are almost unchanged by rescattering, but the helicity of the top quark is strongly affected.

We also consider the momentum average of the polarization

$$\begin{aligned}
 \langle \langle P_L \rangle \rangle &= \frac{4}{3} C_{\perp} \frac{\int_0^{p_{max}} |p G(p, E)|^2 \varphi_R dp}{\int_0^{p_{max}} |p G(p, E)|^2 dp} \\
 &+ \frac{1}{3} k_1 \frac{\int_0^{p_{max}} |p G(p, E)|^2 Re(\Psi_2) dp}{\int_0^{p_{max}} |p G(p, E)|^2 dp},
 \end{aligned} \tag{17}$$

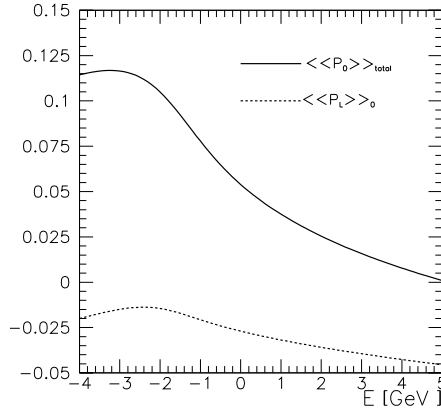


Figure 5: Angular and momentum average of the longitudinal top polarization with rescattering  $\langle\langle\mathcal{P}_L\rangle\rangle$  (solid line), compared with the S-P wave interference term (dashed line).

$$\langle\langle\mathcal{P}_T\rangle\rangle = -\frac{\pi}{4} C_{\parallel}^0 + \frac{\pi}{16} k_2 C_{\parallel}^0 \frac{\int_0^{p_{max}} |p G(p, E)|^2 \Psi_3 dp}{\int_0^{p_{max}} |p G(p, E)|^2 dp}, \quad (18)$$

$$\langle\langle\mathcal{P}_N\rangle\rangle = \frac{\pi}{4} C_N \frac{\int_0^{p_{max}} |p G(p, E)|^2 \text{Im}(\varphi) dp}{\int_0^{p_{max}} |p G(p, E)|^2 dp}. \quad (19)$$

In Fig. 4 we show the drastic change induced by the the final interactions on  $\langle\mathcal{P}_L\rangle$ . The quantity that we wish to compare with [15],  $\langle\langle\mathcal{P}_L\rangle\rangle$  is plotted in Fig. 5. Again we see a substantial change in the normalization and the sign with respect to  $\langle\langle\mathcal{P}_L\rangle\rangle$  from Fig. 3.

For completeness we plot the normal and transverse components of the polarization in Fig. 6 and Fig. 7.

## 4 Conclusions

We have shown that for negative energies relative to the threshold the approximation of [15] does not include the main characteristics of the longitudinal polarization. Even if we neglect the final state interactions the negative energy part is not reproduced. The phenomenological potential changes the

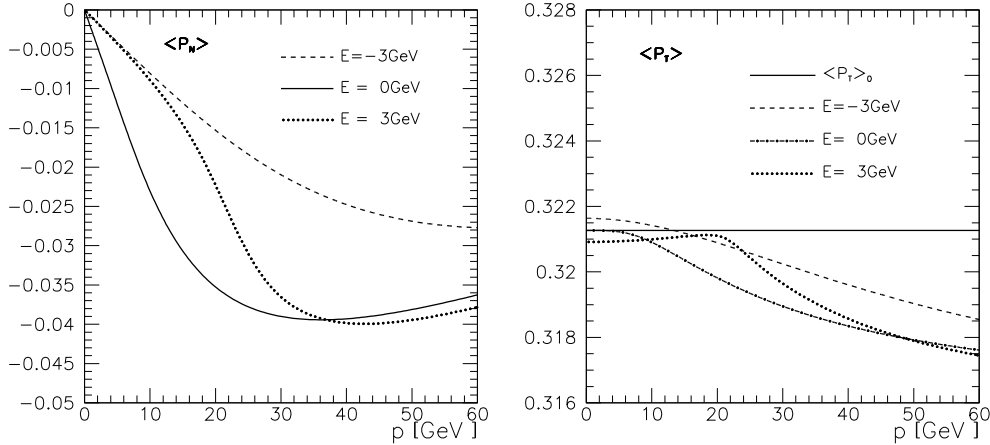


Figure 6: Angular average of the normal  $\langle \mathcal{P}_N \rangle$  (left) and transverse  $\langle \mathcal{P}_T \rangle$  (right) top polarizations plotted for several energies. For  $\langle \mathcal{P}_T \rangle$ , the solid line shows the result without rescattering corrections (which does not depend on energy). The remaining represent the complete result.

normalization slightly, leading to some differences in the positive energy part as well. But our non-relativistic approximation is too crude to seriously improve the predictions of [15] in this region. However a drastic difference appears in a full analysis with the rescattering corrections. It should therefore be obvious that the top quark parameters cannot be retrieved from a fit to Eq. (7) without the inclusion of the rescattering corrections.

Thus the average top quark longitudinal polarization may be a difficult quantity for phenomenological analysis aiming at determination of the top quark couplings. The size of the rescattering corrections should be viewed as an argument against the longitudinal polarization as a source of top parameters. An interesting observable weakly affected by the final state interactions is the forward-backward asymmetry.

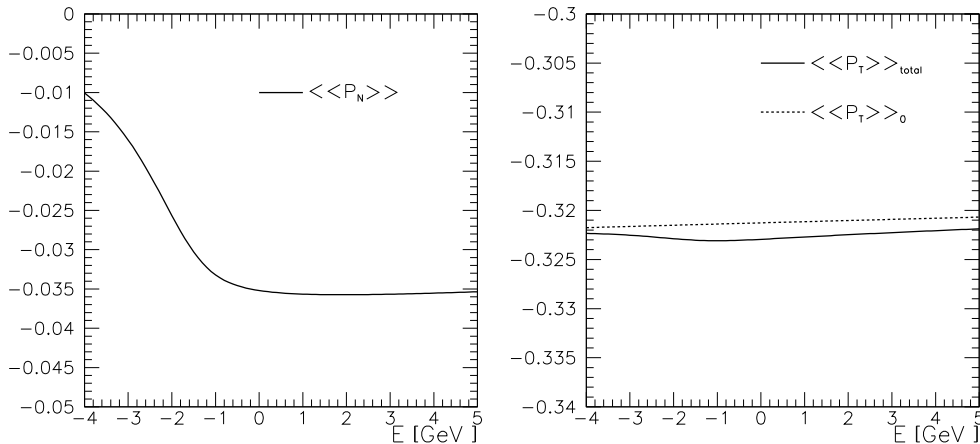


Figure 7: Angular and momentum average of the normal  $\langle\langle\mathcal{P}_N\rangle\rangle$  (left) and transverse top polarization  $\langle\langle\mathcal{P}_T\rangle\rangle$  (right).

## Acknowledgments

The authors wish to thank Thomas Teubner for his support at early stages of this work, helpful comments and careful reading of the manuscript. This work is partly supported by the European Commission 5th Framework contract HPRN-CT-2000-00149 and by KBN grants 5P03B09320 and 2P03B05418.

## A Appendix

Here we would like to show how the results of [9] can be used to calculate the average top quark helicity.

For the definition of the polarization Eq. (1), we need the differential cross section which is equal to

$$\frac{d\sigma}{dp d\Omega_p} d\Omega_p = \frac{d\sigma^{(0)}}{dp} \frac{1}{4\pi} (1 + 2 A_{FB} \cos\vartheta) d\cos\vartheta. \quad (20)$$

$A_{FB}$  is the forward-backward asymmetry

$$A_{FB} = C_{FB} \varphi_R. \quad (21)$$

Then the averaged top polarization is

$$\langle \mathcal{P}_i \rangle = \frac{1}{2} \int_{-1}^1 \mathcal{P}_i (1 + 2 A_{FB} \cos\vartheta) d\cos\vartheta. \quad (22)$$

The unintegrated polarization distributions  $\mathcal{P}_i$ , which are the longitudinal  $\mathcal{P}_L$ , the transverse  $\mathcal{P}_\perp$  and the normal polarization  $\mathcal{P}_N$ , can be easily obtained from the previously calculated polarizations in the beam frame [9] by a rotation of the basis by an angle  $\vartheta$  (the angle between top quark and electron momentum ) in the production plane. Then

$$\begin{aligned} \mathcal{P}_L &= \mathcal{P}_\perp^e \sin\vartheta + \mathcal{P}_\parallel^e \cos\vartheta, \\ \mathcal{P}_T &= \mathcal{P}_\perp^e \cos\vartheta - \mathcal{P}_\parallel^e \sin\vartheta, \\ \mathcal{P}_N &= \mathcal{P}_N. \end{aligned} \quad (23)$$

The index  $e$  was used to indicate that the quantities are given in the basis aligned with the electron momentum. We also use

$$\mathcal{P}_\parallel^e(p, E, \chi) = C_\parallel^0(\chi) + C_\parallel^1(\chi) \varphi_R(\mathbf{p}, \mathbf{E}) \cos\vartheta, \quad (24)$$

$$\mathcal{P}_\perp^e(p, E, \chi) = C_\perp(\chi) \varphi_R(\mathbf{p}, \mathbf{E}) \sin\vartheta, \quad (25)$$

$$\mathcal{P}_N^e(p, E, \chi) = C_N(\chi) \varphi_1(\mathbf{p}, \mathbf{E}) \sin\vartheta. \quad (26)$$

The needed coefficients are [8, 9]

$$\begin{aligned} C_\parallel^0(\chi) &= -\frac{a_2 + \chi a_1}{a_1 + \chi a_2}, & C_\parallel^1(\chi) &= (1 - \chi^2) \frac{a_2 a_3 - a_1 a_4}{(a_1 + \chi a_2)^2}, \\ C_\perp(\chi) &= -\frac{1}{2} \frac{a_4 + \chi a_3}{a_1 + \chi a_2}, & C_N(\chi) &= -\frac{1}{2} \frac{a_3 + \chi a_4}{a_1 + \chi a_2} = -C_{FB}(\chi), \end{aligned} \quad (27)$$

with

$$\begin{aligned} a_1 &= q_e^2 q_t^2 + (v_e^2 + a_e^2) v_t^2 d^2 + 2q_e q_t v_e v_t d \\ a_2 &= 2v_e a_e v_t^2 d^2 + 2q_e q_t a_e v_t d \\ a_3 &= 4v_e a_e v_t a_t d^2 + 2q_e q_t a_e a_t d \\ a_4 &= 2(v_e^2 + a_e^2) v_t a_t d^2 + 2q_e q_t v_e a_t d \\ d &= \frac{1}{16 \sin^2 \vartheta_W \cos^2 \vartheta_W} \frac{s}{s - M_Z^2}. \end{aligned} \quad (28)$$

The following conventions for the fermion couplings are used:  $v_f = 2 I_f^3 - 4 q_f \sin^2 \vartheta_W$ ,  $a_f = 2 I_f^3$ . The parameter  $\chi$  can be interpreted as the effective longitudinal polarization of the virtual intermediate photon or  $Z$  boson:  $\chi = \frac{\mathcal{P}_+ - \mathcal{P}_-}{1 - \mathcal{P}_+ \mathcal{P}_-}$  where  $\mathcal{P}_\pm$  denotes the longitudinal electron/positron polarization.

In an analogous and quite straightforward way the rescattering corrections can be incorporated in our approach; we only have to shift the polarizations  $\mathcal{P}_i \rightarrow \mathcal{P}_i + \delta\mathcal{P}_i$  and the forward-backward asymmetry, as given in [9]. The results are shown in section 2.

## References

- [1] I. Bigi, Y. Dokshitzer, V. Khoze, J. Kühn and P. Zerwas, *Phys. Lett.* **B 181** (1986) 157.
- [2] V. S. Fadin and V. A. Khoze, *JETP Lett.* **46** (1987) 525; *Yad. Fiz.* **48** (1988) 487.
- [3] M. J. Strassler and M. E. Peskin, *Phys. Rev.* **D 43** (1991) 1500.
- [4] Y. Sumino, K. Fujii, K. Hagiwara, H. Murayama and C.-K. Ng, *Phys. Rev.* **D 47** (1993) 56.
- [5] Y. Sumino, PhD thesis, University of Tokyo 1993 (unpublished).
- [6] M. Jeżabek, J. H. Kühn and T. Teubner, *Zeit. Phys.* **C 56** (1992) 653.
- [7] M. Jeżabek and T. Teubner, *Zeit. Phys.* **C 59** (1993) 669.
- [8] R. Harlander, M. Jeżabek, J. H. Kühn and T. Teubner, *Phys. Lett.* **B 346** (1995) 137.
- [9] R. Harlander, M. Jeżabek, J. H. Kühn and M. Peter, *Zeit. Phys.* **C C73** (1997) 477.
- [10] M. Peter and Y. Sumino, *Phys. Rev.* **D 57** (1998) 6912.
- [11] Y. Sumino and M. Jeżabek, *Acta Phys. Polonica* **B 29** (1998) 1443.
- [12] M. Jeżabek, *Acta Phys. Polonica* **B 26** (1995) 789.

- [13] T. Teubner, *Acta Phys. Polonica* **B 30** (1999) 1941.
- [14] E. Accomando *et al.*, *Phys. Rept.* **299** (1998) 1-78.
- [15] B. M. Chibisov, M. B. Voloshin, *Mod. Phys. Lett. A* **13** (1998) 973-978.
- [16] A. H. Hoang, T. Teubner, *Phys. Rev. D* **60** (1999) 114027.
- [17] A. H. Hoang *et al.*, *Eur. Phys. J. Direct C* **3** (2000) 1.
- [18] A. H. Hoang, A. V. Manohar, I. W. Stewart and T. Teubner, *Phys. Rev. Lett.* **86** (2001) 1951-1954.
- [19] V. S. Fadin, V. A. Khoze and M. I. Kotsky, *Zeit. Phys. C* **64** (1994) 45.